Lattice Boltzmann simulation of two-phase magmatic flows using Immersed Boundary method

Yann Thorimbert*[1], Francesco Marson[1], Andrea Parmigiani[2], Bastien Chopard[1] and Jonas Lätt[1]

[1]Department of Computer Science, University of Geneva
[2]Department of Earth Sciences, ETH Zürich

October 31, 2017

Abstract

We present a lattice Boltzmann model designed for the simulation of dilute and dense finite-sized rigid particle suspensions, aiming at studying the rheology of crystal bearing magma that flows under applied shear.

We use a bottom-up approach and fully resolve the mechanical interaction between fluid and particles. Our model consists in coupling a lattice Boltzmann scheme for Newtonian and incompressible fluid flows with an immersed boundary scheme to simulate two-ways fluid-particles interaction. We introduce a simple yet robust contact model that includes repulsive elastic collision between particles, and neglects lubrication corrections. We apply this model to simple sheared flow with rigid spherical particles and we provide results for the relative apparent viscosity of the particle suspension as a function of the particle volume fraction and strain rate of the flow.

We find that, using the proposed approach, there is no need for a lubrication model in the magmatic regime, provided that an elastic contact model is included. Our algorithm, therefore, can be based only on physically sound and simple rules, a feature that we think to be fundamental for aiming at resolving polydispersed and arbitrarily shaped particle suspensions, as those found in magmatic environments.

Comparing our results with Krieger-Dougherty semi-empirical law, we demonstrate that the simulations are not sensitive to the particle

*yann.thorimbert@unige.ch, Battelle - batiment A, 7 route de Drize, CH-1227 Carouge

Reynolds number for $Re_p \ll 1$, which is the Reynolds of interest for modeling magmatic flows.

We show that the proposed model is sufficient to obtain a correct description of the rheology of particle suspension up to volume fraction equal to 0.55 (approaching the critical random packing fraction for monodispersed spheres), which goes beyond the state of the art. We finally demonstrate that the fluid-solid density ratio does not impact significantly the simulations in absence of gravity, which allows us to increase the performance and stability of the implemented algorithm.

Keywords— lattice Boltzmann, particle suspensions, magmatic flow, immersed boundary method, numerical rheology

1 Introduction

Magma is a multicomponent mixture of silicate melt and crystals (*i.e.* crystals bearing magma) that, at shallow levels in the crust, can experience the exsolution of volatiles and form a three phase suspensions (*i.e.* crystals and bubbles bearing magma). The rheology of crystal bearing magmas has been extensively investigated experimentally and it has been found that magma exhibits non-Newtonian behavior at both high particle volume fraction ϕ and/or strain rate $\dot{\gamma}$ (see [35, 26]). Experimental investigations focused on determining the rheology of bubbles and crystals bearing magmas also exists (refer to [26] for instance). However the complex non-linear interaction between the three coexisting phases substantially increase the complexity of magma rheology characterization. In this context, numerical modeling of particles and bubbles suspensions aimed at directly/fully resolving the mechanical interaction between the different phases at the scale of bubbles and crystals may reveal fundamental to improve our understanding of magma rheology.

As a first step to build such a tool, a two-phase (fluid and particles) scenario is considered in this article. In particular, to validate our approach, it is crucial that the rheological behavior of the simulated particle suspension follows the Krieger-Dougherty law [16], that relates the relative apparent viscosity μ_r of the suspension to the particle volume fraction ϕ as:

$$\mu_r = \left(1 - \frac{\phi}{\phi_M}\right)^{-B\phi_M}, \tag{1}$$

with ϕ_M the maximum packing fraction. Throughout all this study, we used $B = 2.5$, which is a common value for rigid spheres [7, 36, 37, 12]. Equation 1 is widely used and proves to be in good correlation with experimental data [7, 28, 26].

Moreover, in order to model particle suspensions that mimic a magmatic environment, one should reproduce as much as possible a viscous (particle Reynolds number, $Re_p \ll 10^{-3}$), strongly coupled (Stokes number, $St \ll 1$) and hydrodynamic (Peclet number, $Pe \gg 10^3$) regime [26]. The particle Reynolds number of a suspension Re_p is defined as $Re_p = \rho_f r^2 \dot{\gamma}/\mu_0$, where ρ_f is the density of the suspending fluid phase, r is the particle radius, $\dot{\gamma}$ is the strain rate and μ_0 the viscosity of the pure fluid phase. Similarly, using the density ρ_s of the solid phase (particles), the Stokes number of the flow reads $St = \rho_s r^2 \dot{\gamma}/\mu_0$ and characterizes the coupling between solid and fluid phases. Finally, the Peclet number $Pe = 6\pi\mu_0 r^3 \dot{\gamma}/(kT)$ accounts for the effect of Brownian motion of suspended particles, with k the Boltzmann constant and T the temperature.

Particle suspension dynamics is often simulated including rheological parametrization for non-Newtonian fluids into Navier-Stokes equations (see [27, 15, 39]). Our goal here is to develop a more fundamental model, in which the non-Newtonian viscosity of the suspension emerges naturally from the interaction between a Newtonian fluid (*i.e.* the melt) and the particles it contains (*i.e.* the crystals). LB is a well suited technique for reaching such a goal due to its capability to deal with complex physics and geometry (see [33, 41] for instance). Indeed, our choice of LB method is dictated by our desire to eventually develop a three phase magma model, for instance two immiscible fluids (where LB is known to excel [32]) interacting with moving solid particles.

To the best of authors' knowledge, LB works targeted to model particle suspension under magmatic flows conditions do no exist. However, many LB works aiming at achieving direct numerical simulation of particles suspensions have been published and several are the methods proposed to simulate moving solid boundaries. In [20, 21, 2], a generalization of the bounce-back rules for moving boundaries is developed. The immersed boundary (IB) method ([34, 40]), based on a Lagrangian point of view, is an alternative that is increasing in popularity [44, 29]. In the present paper, we focus on a multi-direct forcing approach of IB which has recently been adapted to the field of LB methods [30] and that we think particularly well suited to the case where multiphase fluid phases may interact with each other and the solid particles.

In the LB literature for particle suspensions, excellent agreement with theory has been reported in [12] for $\phi < 0.5$. In [23], the authors investigate particle suspension up to $\phi < 0.2$. On the same line, [19] simulate suspensions with $\phi \leq 0.3$. While the aforesaid works all use rigid spheres as suspended particles, [25], coupling LB to a finite-element method for particle deformation, simulate deformable spheres as well as blood platelets and obtain good results for $\phi < 0.5$. In [13], a wide range of particle shapes are simulated and shows good agreement

with other authors, and different lubrication models are compared.

Probably due to its less straightforward implementation, the IB method has been used more sporadically in this field. In [17] good results using IB method for spherical and deformable platelets particles are presented, while [4] apply it to a large number of spherical particles, yielding correct results for $\phi < 0.4$.

Some of the aforementioned LB studies obtain good agreement with the experimental data. However, for what concerns the relative apparent viscosity μ_r as a function of ϕ, it seems still difficult to properly model the case of very high particle concentrations, where ϕ is approaching the maximum packing fraction ϕ_M ($\phi_M \approx 0.64$ in the case of spheres). In particular, no work reports convincing results for $\phi > 0.5$. The investigation of such relationship is one of the main goals of this work.

Finally, in [7], it is stressed that slight differences in the hypotheses on which the contact and/or lubrication model are based result in substantially different outputs. A similar observation is done in [38], where the authors remark how, at high particle volume fraction, models results are extremely sensitive to nonhydrodynamic interparticle forces. The authors conclude, therefore, that the most crucial point for a successful particle suspension simulation is to employ a proper contact model. This point of view is supported by several works studying the impact of interparticle interaction on suspensions rheology. Therefore, it seems to be critical to us to be able to achieve realistic simulations using a minimum number of modeled ingredients.

2 Method

In this work we resolve the Navier-Stokes equations for an incompressible fluid using a Bhatnagar-Gross-Krook (BGK) single relaxation time collision model [3] with a D3Q19 topology. We used the Palabos open-source library [31] for all the simulations presented.

Many physical properties of magma are difficult to simulate: in the context of this work, the most extreme one is the high viscosity of the silicate melt (from 10^{-1} Pa $\cdot$ s to 10^{6} Pa $\cdot$ s approximately, depending on the melt composition [5]) that makes the flow Reynolds number Re extremely low. Indeed, for $Re \ll 1$ and for fixed lattice spacing Δx and relaxation time τ, the lattice time step Δt has to be kept very small because τ is directly related to the viscosity. Discussions on the scaling of Δt for low Re can be found in [17, 18]. In this study, we kept the value $\tau = 1$ and adapted Δt consequently (see Section 2.4 for a detailed description of the parameters).

2.1 Fluid-Solid coupling

Here we represent particles as rigid bodies whose motion, in absence of particle-particle interaction, follows the classical laws of mechanics as determined solely by the interaction between the fluid and a solid body. We model that by using the multi-direct forcing IB scheme ([43]), following the implementation presented in [30].

As a benchmark for our implementation, we used Jeffery's solution for the angular velocity $\dot{\varphi}$ of an ellipsoid with aspect ratio r_e in a shear flow with strain rate $\dot{\gamma}$ [14]:

$$\dot{\varphi} = \frac{\dot{\gamma}}{r_e^2 + 1} \left(r_e^2 \cos^2 \varphi + \sin^2 \varphi \right), \tag{2}$$

and the period T of the ellipsoid reads $T = 2\pi(r_e + 1/r_e)/\dot{\gamma}$.

In Figure 1, we show the normalized angular velocity $\dot{\varphi}T/2\pi$ about the vorticity vector for several different ellipsoids simulated with our IB implementation against the reference solution.

2.2 Contact model

A common approach (see [12, 38, 6, 13] for instance) to the modeling of particle-particle interaction makes use of two steps: 1) a lubrication model, which is a sub-grid model accounting for the non-resolved pure hydrodynamic effect of increasing repulsive force, that a particle experience while it approaches another solid boundary [8], and 2) an additional contact model for very close particles, supplying the lubrication model, which fails for very small gap between boundaries [7, 12, 13]. In some cases a third, non-physical model for extremely close or interpenetrating particles is also used [12].

We think that this general approach to model the collisions is not necessarily the best one. In the case of magmatic flows indeed, the use of a lubrication subgrid model appears superfluous and we will show how a simple repulsive soft-collision elastic model (step 2 only) is sufficient to recover a realistic suspension behavior.

The repulsive spring model we use reads as follow. We consider spherical particles 1 and 2, whose center are denoted by $\mathbf{x}_1$ and $\mathbf{x}_2$ respectively. The corresponding radii are named r_1 and r_2, so the gap between particles reads $h = \|\mathbf{x}_1 - \mathbf{x}_2\| - r_1 - r_2$. The force exerted by particle 1 on particle 2 is then equal to

$$\mathbf{F}_{12} = -\mathbf{F}_{21} = \begin{cases} -k(\delta - h)\frac{\mathbf{x}_2 - \mathbf{x}_1}{\|\mathbf{x}_2 - \mathbf{x}_1\|} & \text{if } h < \delta \\ 0 & \text{otherwise,} \end{cases} \tag{3}$$

with k and δ some parameters of the force model whose impact is discussed below. This method is general and may be applied to

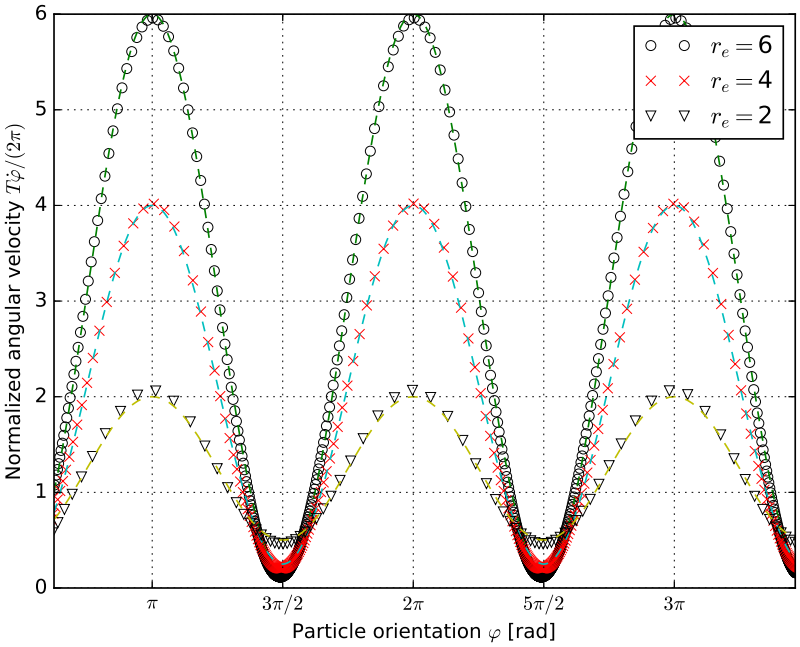

Figure 1: Normalized angular velocity $\dot{\varphi}T/2\pi$ about the vorticity vector for several spheroidal particles with aspect ratio r_e in a shear flow, as a function of particle orientation, for a strain rate $\dot{\gamma} = 10^3\, s^{-1}$. Simulation points are compared to Jeffery's analytical solution (dashed lines).

particles of arbitrary shape, except for the space gap between particles and the orientation of the applied forces, which should be computed accordingly.

A consequence of the used model is that a slight particle interpenetration can occur during collisions. Using Equation 3, the work done by a moving particle interpenetrating a rest particle by a distance D can be calculated as

$$W = \int_{\delta}^{\delta - D} F(x)\ dx = k\frac{D^2}{2}. \tag{4}$$

If the kinetic energy of the incoming particle is given by $E = mu^2/2$, it follows that the interpenetration distance can be expressed as $D = u\sqrt{m/k}$, with m and u the mass of the particle and the characteristic velocity of the flow respectively. Given D, which must be much smaller than the typical particle radius r, one determines the value of k. Note that D impacts the actual volume fraction, since the particles collide with an effective radius equal to $r - D$ (if one chooses $\delta = 0$). Thus, the effective volume fraction ϕ must be computed using this effective radius. For $D = r/100$, this reduces the volume fraction by three percent approximately.

As a final remark, one should ensure that $D \gg u \cdot \Delta t$; this is to say the time step is small enough for the spring collisions to be sufficiently resolved in time. For the typical simulation configuration used in this study (see Section 2.4), this leads to $\Delta t \ll 10^{-5}$, which is consistent with the time step already required by the type of flow simulated (see Section 2.4). However, for smaller values of D (*i.e* larger spring constant k), one should adapt the time step consequently.

2.3 Viscosity measurement

As reported in [1], different methods can be exploited to compute apparent viscosity of suspensions. In some flow configurations, spurious viscosity can appear near the walls, giving rise to the so-called wall effect. A convenient way to avoid wall effect is to use Lees-Edwards boundary conditions [24, 42] in order to emulate an infinite domain along the axis on which the velocity gradient is applied. This method has been used by [23] for instance, who then relates the viscosity to the total dissipation of the fluid. It is also possible, as in [17] for example, to integrate the fluid stress tensor over particles surfaces. For the type of flow considered in this work, the results indicate that the wall effect can be ignored, as done in [12]. Moreover, this effect is also present in laboratory experiments [7]. For this reason, we used an evaluation of the average wall shear stress at the walls in order to compute the viscosity of the simulated suspensions. As indicated by [17], this method is sufficient as long as local stresses assessment can be avoided.

2.4 Simulation setup

The simulation setup we choose is inspired and consistent with those of a real rheometer as described in [28]. Flow and particles parameters reflect magma properties as reported in [26].

Other model parameters are chosen to guarantee stability and accuracy, as discussed in the above subsections. No gravity is applied. It has been observed that the lattice spacing Δx must be approximately ten times smaller than the particle radius r in order to obtain accurate results (see Section 3.2). The typical number of particles simulated in the concentrated regime is approximately 10^3. Simulations with up to 10^4 particles were achieved and yielded similar results. Table 1 summarizes the typical values used for the simulations.

The Stokes and Peclet number are $St = 10^{-2}$ and $Pe = 10^{11}$ respectively, which corresponds well to the magmatic regime as discussed in the introduction ($St \ll 1$ and $Pe \gg 10^3$). However, the particle Reynolds number corresponding to these parameters is $Re_p = 10^{-2}$, which is too large to characterize a flow completely dominated by viscous forces. As mentioned above, this is due to the fact that the time step Δt directly relates to the viscosity of the fluid, resulting in reduced performances for highly viscous flows. Instead of overcoming this issue by using greater computational resources, one can argue that, as in [18, chap. 7.2.3.3] for instance, Re_p is still sufficiently small for the flow to be insensitive to its actual value. This allow us to use a numerical Reynolds number larger than the physical one in order to speed up the simulations. The validity of this assumption is demonstrated in the results section in Figure 3.

Figure 2 illustrates a possible simulation configuration. Periodic boundary conditions are used along the x and z axes, while velocity boundary conditions $u_x(x, 0, z) = l_y\dot{\gamma}$ and $u_x(x, l_y, z) = 0$ are imposed using a regularized scheme as proposed in [22].

3 Results

Figure 3 shows apparent relative viscosity results as a function of the volume fraction of particles for different simulations (the standard configuration as described in Table 1 is used). Each point corresponds to a different simulation in which the spherical particles are randomly placed in the domain at the beginning of the simulation. This was done for different particle Reynolds number Re_p. It is found that the results in the range $10^{-3} \leq Re_p \leq 10^{-1}$ are similar. Numerical apparent relative viscosity is in good agreement with Equation 1 up to $\phi = 0.54$. The results are also compared to Einstein's model [9, 10], who demonstrated that the relationship $\mu_r = 1 + 2.5\phi$ holds for a Newtonian suspension of dilute spherical particles.

Table 1: Summary of the typical value for the main parameters of the simulations.

Parameter	Unit	Name	Value
Domain length	[m]	l_x	10^{-2}
Domain height	[m]	l_y	10^{-3}
Domain width	[m]	l_z	$2 \cdot 10^{-3}$
Lattice time step	[s]	Δt	$6 \cdot 10^{-7}$
Lattice spacing	[m]	Δx	$2 \cdot 10^{-5}$
Particle radius (when spherical)	[m]	r	10^{-4}
Fluid viscosity (without particles)	[Pa · s]	μ_0	10^{-1}
Fluid density	[kg · m^{-3}]	ρ_f	10^3
Solid density	[kg · m^{-3}]	ρ_s	$2 \cdot 10^3$
Strain rate	[s^{-1}]	$\dot{\gamma}$	$10^{\ 2}$
Interpenetration parameter	[m]	D	10^{-6}
Spring constant	[N · m^{-1}]	k	1

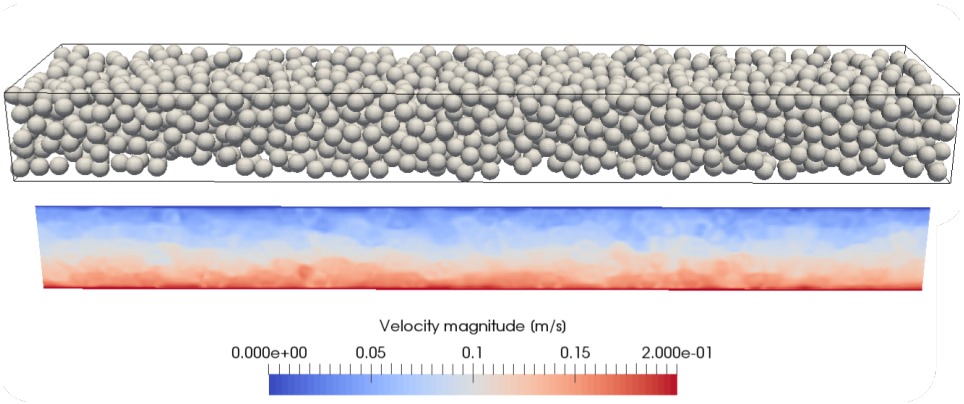

Figure 2: (top) Example of a simulation with $\phi = 0.4$ and (bottom) the corresponding velocity magnitude at the center of the domain.

Literature results based on laboratory experiments show that a critical volume fraction ϕ_c exists above which continuous networks of interconnected particles (*i.e.* chains of particles) can form. For uniform distribution of solid spheres, this value is between 0.5 and 0.55 [7]. Our model is able to produce accurate results up to ϕ_c, while it fails for larger values. As can be deduced from the fact that existing studies using direct simulation methods all provide results for $\phi < 0.5$ (see the introduction section), it is likely that the critical volume fraction constitutes a limitation for any numerical model which does not employ a method specifically devoted to the treatment of chains of particles, as the borderline with granular media is reached, and jamming transitions occur [28].

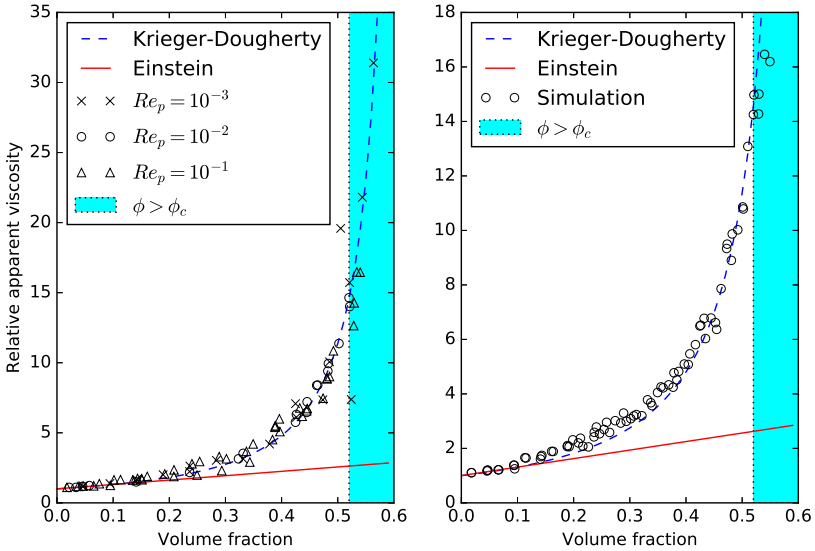

Figure 3: Relative apparent viscosity as a function of the volume fraction for randomly initialized spheres of equal radius. (left) The results are found to be similar for various particle Reynolds number Re_p. (right) Results from the simulations setup corresponding exclusively to the configuration of Table 1. All the results are compared to Krieger-Dougherty and Einstein laws. The colored area represents the concentrations range that is above the critical volume fraction ($\phi_c \approx 0.52$).

Figure 4 displays, for several values of ϕ, the shear stress as a function of the strain rate, as compared to Krieger-Dougherty law. These simulations have been performed for numerous values of strain

rate. We thus demonstrate the accuracy and robustness of the model for a range of shear flows, up to values of strain rate inducing non-Newtonian behavior.

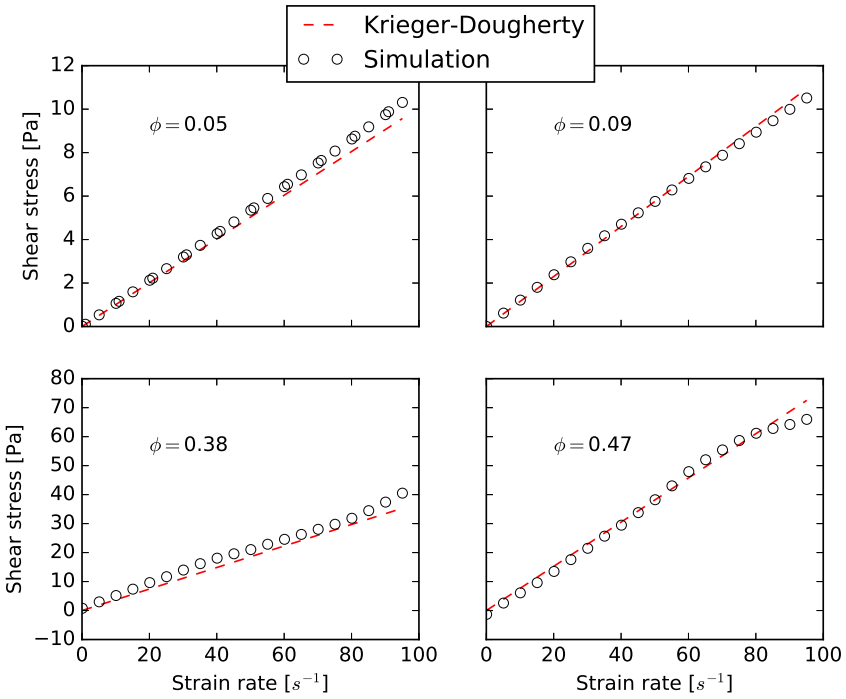

Figure 4: Shear stress as a function of the strain rate for randomly initialized spheres of equal radius. The accuracy of the model is validated for a wide range of strain rates, up to non-Newtonian behavior.

It must be noted that all the results presented above have been obtained without a lubrication model. As also numerically verified by [13, 37], in a dilute regime (*i.e.* when $\phi < 0.2$) it is practicable to not use any contact nor lubrication model (see Figure 5). This because the lattice Boltzmann model correctly recovers the hydrodynamical interaction between approaching particles when the gap between them is larger than one lattice cell.

For more dense particle suspensions instead, both accuracy and numerical stability are strongly impacted by particle-particle interactions, and a contact or lubrication model is obviously needed. As also reported in [11, 13], the exact value of the spring model does not impact the rheological behavior, as long as k (or D) is properly adapted to the flow properties, as discussed in Sect. 2.2.

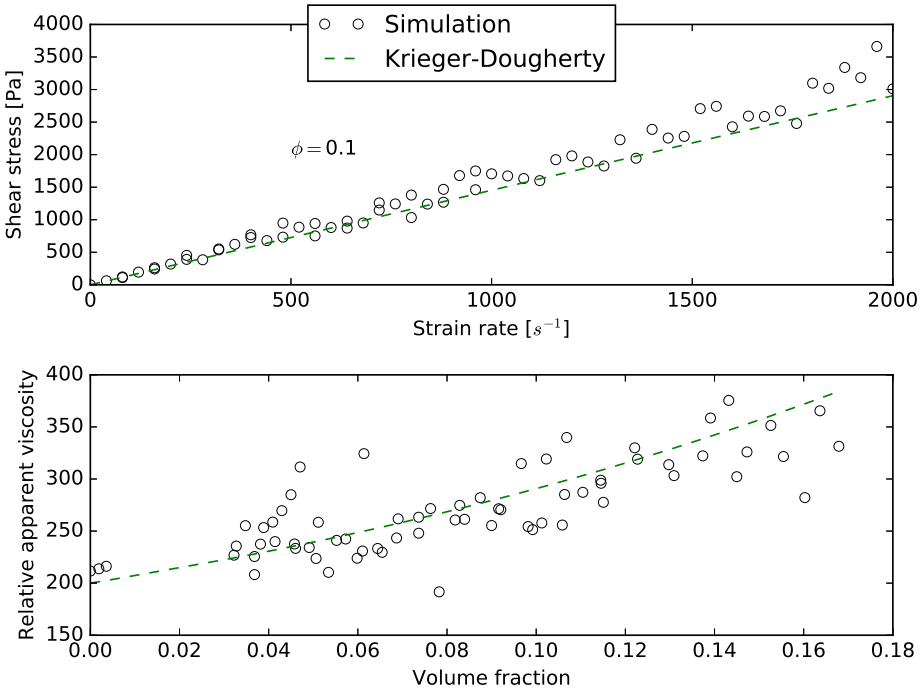

Figure 5: Example of results obtained interparticle interaction model, for shear stress as a function of the strain rate with $\phi = 0.1$ (top) and relative apparent viscosity as a function of the volume fraction (bottom), showing that, up to $\phi \approx 0.2$, no particle-particle interaction model is needed.

3.1 Influence of the density ratio

As noted by [37], numerical instabilities can appear when the density ρ_s of the solid particles is close to the density ρ_f of the fluid. It is therefore of interest to show that the results are not dependent of the density ratio, so that one can perform simulations with $\rho_s/\rho_f > 1$. For instance, [45] uses a density ratio equals to 10, while it is equal to 3.5 in [37].

In Figure 6 we demonstrate that the density ratio does not have a significant impact on the results in the range $1.3 \leq \rho_s/\rho_f \leq 6$, in accordance with the results of [37] in which a derivative of Ladd's method is used, indicating that this phenomenon does not only occur with IB methods. For this reason, our simulations were performed with a density ratio equal to 2 in order to improve stability.

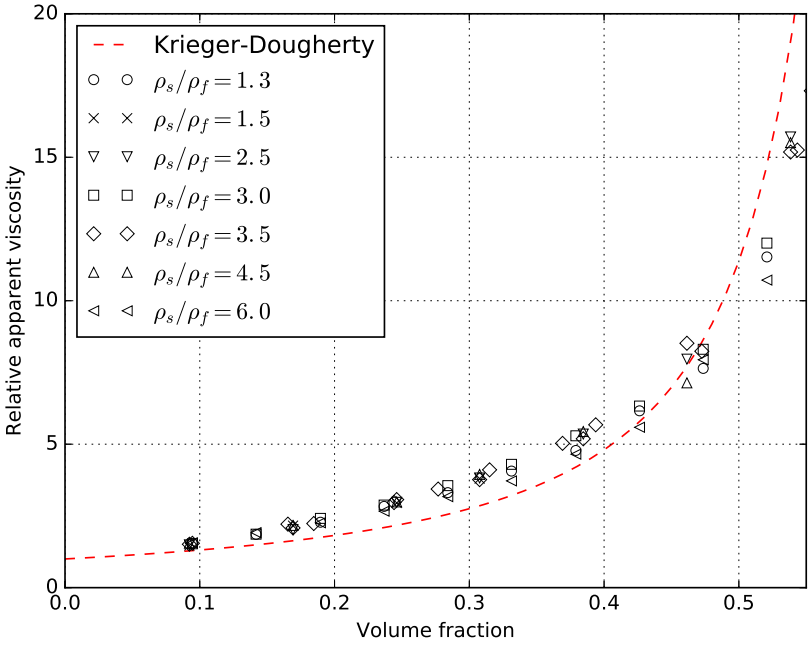

Figure 6: Influence of the solid-fluid density ratio ρ_s/ρ_f on the relative apparent viscosity as a function of the volume fraction ϕ.

3.2 Grid convergence of the model

Simulations have been performed for several values of Δx in order to study the evolution of the accuracy as the lattice spacing is refined. We define the relative error as $\epsilon = |\mu_r - \mu_r^{ref}|/\mu_r^{ref}$. The reference solution μ_r^{ref} corresponds to the Krieger-Dougherty law. Figure 7 shows the relative apparent viscosity and the mean relative error as a function of Δx, for two different configurations at high volume fraction. It is found that the order of convergence is $\mathcal{O}(\Delta x)$. We also conclude that, in order to achieve $\epsilon \approx 5\%$ for any particle concentration, one needs to use a lattice spacing approximately ten times smaller than the particle diameter.

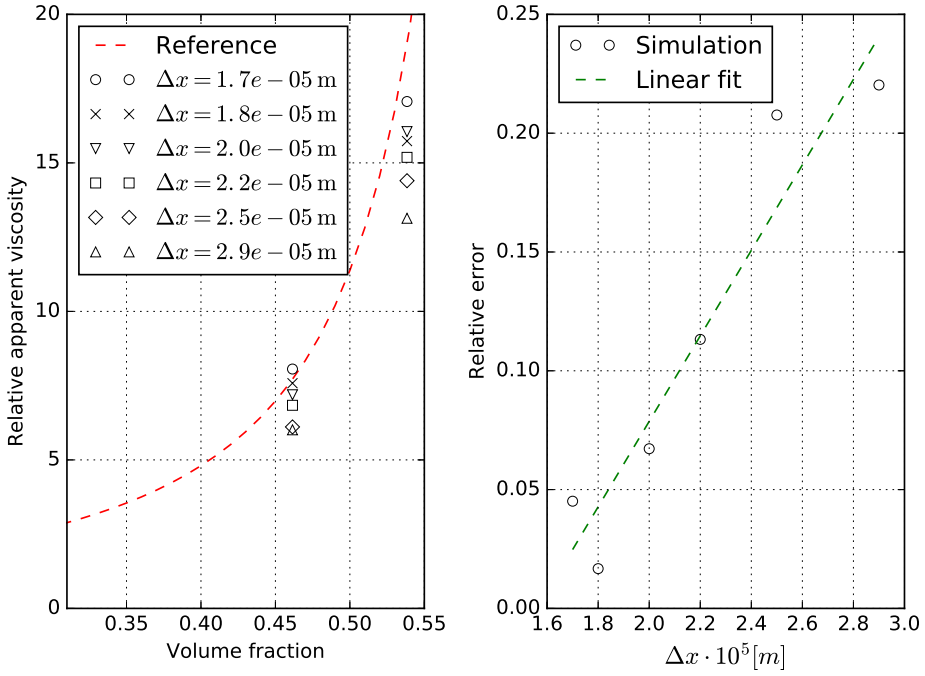

Figure 7: (left) Relative apparent viscosity as a function of the volume fraction for several values of lattice spacing and (right) relative error as a function of the lattice spacing. The order of convergence of our model is $\mathcal{O}(\Delta x)$.

4 Conclusions

We presented a LB-IB model especially suited to investigate the rheology of spherical and rigid particle suspensions flowing under magmatic conditions (viscous, strongly coupled and hydrodynamic regime, as said in the introduction). Particle-particle interactions are solved employing a contact-model only (no lubrication model is used), but yet our results are in excellent agreement with Krieger-Dougherty law for both dilute and dense particle suspension up to the critical random packing fraction where particle chains are likely to form ($\phi_c \approx 0.55$ for monodispersed rigid spheres).

There are two main contributions in this work. Firstly, we show that a lubrication model is not necessarily required to achieve realistic results for dense particle suspension rheology at $Re_p \ll 1$. In a future work, the exact reason for this result should be further investigated through a detailed analysis of the interaction between the suspension components, as it may bring an improved understanding of the collision mechanisms in suspensions.

A second interesting observation we make concerns the insensitivity of the results to the particle Reynolds number in the range $10^{-3} \leq Re_p \leq 10^{-1}$ and to the solid-fluid density ratio in the range $1.3 \leq \rho_s/\rho_f \leq 6$. The implication of this observation are multiple; indeed numerical stability can be potentially improved by using larger density ratios as long as particle's buoyancy to be simulated is null, and higher simulation performance can be reached employing a numerical particle Reynolds number larger than the physical one and, fundamental to us, still recover the correct rheological behavior of highly viscous crystal bearing magmatic suspensions.

Future challenges for our work focus on better modeling particle suspensions in magmatic environments. Our priority is to introduce polydispersed cuboidal shaped particles with aspect ratios and size distributions similar to the one of igneous crystals. To model appropriate size distributions and provide statistical meaningful results will require a large computational domain and potentially a large number of particles (especially smaller ones). For this reason, particular attention should be given to the parallelization efficiency of the implementation.

Finally, it is worth mentioning that the yield stress of the suspension was not treated in this study, though it constitutes an important feature of suspensions in concentrated regimes. As noted by [17], instead of applying a strain rate to the fluid by imposing velocity boundary conditions, one should rather impose a shear stress at the boundaries and observe the suspension velocity in order to discern the yield stress. We plan to perform such an analysis in a more detailed study dedicated to the rheology of magma-like suspensions.

Acknowledgments

The research leading to these results has received support from the Swiss National Science Foundation.

We also thank CADMOS for financial support.

The computations were performed at the University of Geneva on Scylla cluster.

References

[1] Cyrus K. Aidun and Jonathan R. Clausen. Lattice-boltzmann method for complex flows. *Annual Review of Fluid Mechanics*, 42(1):439–472, 2010.

[2] Cyrus K. Aidun and Yannan Lu. Lattice boltzmann simulation of solid particles suspended in fluid. *Journal of Statistical Physics*, 81(1):49–61, Oct 1995.

[3] P. L. Bhatnagar, E. P. Gross, and M. Krook. A model for collision processes in gases. *Phys. Rev.*, 94:511–525, 1954.

[4] Simon Bogner. *Direkte Numerische Simulation von Flüssig-Gas-Feststoff - Strömungen basierend auf der Lattice Boltzmann-Methode*. PhD thesis, 2017.

[5] Y. Bottinga and D. F. Weill. The viscosity of magmatic silicate liquids; a model calculation. *American Journal of Science*, 1972.

[6] Jonathan R Clausen. *the Effect of Particle Deformation on the Rheology and Microstructure of Noncolloidal Suspensions the Effect of Particle Deformation on the Rheology and Microstructure of*. PhD thesis, Georgia Institute of Technology, 2010.

[7] P. Coussot and C. Ancey. Rheophysical classification of concentrated suspensions and granular pastes. *Physical Review E*, 1999.

[8] R.G. Cox. *The motion of suspended particles almost in contact*. International Journal of Multiphase Flow. 1974.

[9] A. Einstein. Eine neue bestimmung der moleküldimensionen. *Annalen der Physik*, 324(2):289–306, 1906.

[10] A. Einstein. Berichtigung zu meiner Arbeit: Eine neue Bestimmung der Moleküldimensionen. *Annalen der Physik*, 34:591–592, 1911.

[11] Zhi-Gang Feng and Efstathios E Michaelides. The immersed boundary-lattice boltzmann method for solving fluid–particles interaction problems. *Journal of Computational Physics*, 195(2):602 – 628, 2004.

[12] J. Hyväluoma, P. Raiskinmäki, A. Koponen, M. Kataja, and J. Timonen. Lattice-Boltzmann simulation of particle suspensions in shear flow. In *Journal of Statistical Physics*, 2005.

[13] F. Janoschek. *Mesoscopic simulation of blood and general suspensions in flow*. PhD thesis, Eindhoven University of Technology, 2013.

[14] G B Jeffery. The Motion of Ellipsoidal Particles Immersed in a Viscous Fluid. *Proceedings of the Royal Society of London A: Mathematical, Physical and Engineering Sciences*, 102(715):161–179, 1922.

[15] Safoora Karimi, Mahsa Dabagh, Paritosh Vasava, Mitra Dadvar, Bahram Dabir, and Payman Jalali. Effect of rheological models on the hemodynamics within human aorta: Cfd study on ct image-based geometry. *Journal of Non-Newtonian Fluid Mechanics*, 207:42 – 52, 2014.

[16] Irvin M. Krieger and Thomas J. Dougherty. A mechanism for non-newtonian flow in suspensions of rigid spheres. *Transactions of the Society of Rheology*, 3(1):137–152, 1959.

[17] T. Krüger. *Computer Simulation Study of Collective Phenomena in Dense Suspensions of Red Blood Cells under Shear*. Vieweg+Teubner Verlag, 2012.

[18] T. Krüger, H. Kusumaatmaja, A. Kuzmin, O. Shardt, G. Silva, and E.M. Viggen. *The Lattice Boltzmann Method: Principles and Practice*. Graduate Texts in Physics. Springer International Publishing, 2016.

[19] Pandurang M. Kulkarni and Jeffrey F. Morris. Suspension properties at finite reynolds number from simulated shear flow. *Physics of Fluids*, 20(4):040602, 2008.

[20] Anthony J. C. Ladd. Numerical simulations of particulate suspensions via a discretized boltzmann equation. part 1. theoretical foundation. *Journal of Fluid Mechanics*, 271:285–309, 1994.

[21] Anthony J. C. Ladd. Numerical simulations of particulate suspensions via a discretized boltzmann equation. part 2. numerical results. *Journal of Fluid Mechanics*, 271:311–339, 1994.

[22] Jonas Latt, Bastien Chopard, Orestis Malaspinas, Michel Deville, and Andreas Michler. Straight velocity boundaries in the lattice boltzmann method. *Phys. Rev. E*, 77:056703, May 2008.

[23] S. V. Lishchuk, I. Halliday, and C. M. Care. Shear viscosity of bulk suspensions at low reynolds number with the three-dimensional lattice boltzmann method. *Phys. Rev. E*, 74:017701, Jul 2006.

[24] Eric Lorenz, Alfons G. Hoekstra, and Alfonso Caiazzo. Lees-edwards boundary conditions for lattice boltzmann suspension simulations. *Phys. Rev. E*, 79:036706, Mar 2009.

[25] Robert M. MacMeccan, J. R. Clausen, G. P. Neitzel, and C. K. Aidun. Simulating deformable particle suspensions using a coupled lattice-boltzmann and finite-element method. *Journal of Fluid Mechanics*, 618:13–39, 2009.

[26] H. M. Mader, E. W. Llewellin, and S. P. Mueller. The rheology of two-phase magmas: A review and analysis. *Journal of Volcanology and Geothermal Research*, 257:135–158, May 2013.

[27] O. Malaspinas, N. Fiétier, and M. Deville. Lattice boltzmann method for the simulation of viscoelastic fluid flows. *Journal of Non-Newtonian Fluid Mechanics*, 165(23):1637 – 1653, 2010.

[28] S. Mueller, E. W. Llewellin, and H. M. Mader. The rheology of suspensions of solid particles. *Proceedings of the Royal Society of London A: Mathematical, Physical and Engineering Sciences*, 466(2116):1201–1228, 2010.

[29] Yuichi Nakatani, Kosuke Suzuki, and Takaji Inamuro. Flight control simulations of a butterfly-like flapping wing–body model by the immersed boundary–lattice boltzmann method. *Computers and Fluids*, 133(Supplement C):103 – 115, 2016.

[30] Keigo Ota, Kosuke Suzuki, and Takaji Inamuro. Lift generation by a two-dimensional symmetric flapping wing: immersed boundary-lattice boltzmann simulations. *Fluid Dynamics Research*, 44(4):045504, 2012.

[31] Palabos. `http://www.palabos.org`. Online; accessed 30 october 2017.

[32] A. Parmigiani, W. Degruyter, S. Leclaire, C. Huber, and O. Bachmann. The mechanics of shallow magma reservoir outgassing. *Geochemistry, Geophysics, Geosystems*, 18(8):2887–2905, 2017.

[33] Andrea Parmigiani, Jonas Latt, Mohamed Ben Belgacem, and Bastien Chopard. A lattice Boltzmann simulation of the Rhone river. *Int. J. Mod. Phys. C*, 24(11):1340008, 2013.

[34] Charles S Peskin and To Dora. The immersed boundary method. *Acta Numerica*, pages 479–517, 2002.

[35] N. Petford. Which effective viscosity? *Mineralogical Magazine*, 73(2):167–191, 2009.

[36] P. Raiskinmäki, A. Shakib-Manesh, A. Koponen, A. Jäsberg, M. Kataja, and J. Timonen. Simulations of non-spherical particles suspended in a shear flow. *Computer Physics Communications*, 2000.

[37] A. Shakib-Manesh, P. Raiskinmäki, A. Koponen, M. Kataja, and J. Timonen. Shear stress in a Couette flow of liquid-particle suspensions. In *Journal of Statistical Physics*, 2002.

[38] A Sierou and J F Brady. Rheology and microstructure in concentrated noncolloidal suspensions. *Journal of Rheology*, 46(5):1031–1056, 2002.

[39] Anastasios Skiadopoulos, Panagiotis Neofytou, and Christos Housiadas. Comparison of blood rheological models in patient specific cardiovascular system simulations. *Journal of Hydrodynamics, Ser. B*, 29(2):293 – 304, 2017.

[40] Kosuke Suzuki and Takaji Inamuro. Effect of internal mass in the simulation of a moving body by the immersed boundary method. *Computers and Fluids*, 49(1):173–187, 2011.

[41] Y. Thorimbert, J. Latt, L. Cappietti, and B. Chopard. Virtual wave flume and Oscillating Water Column modeled by lattice Boltzmann method and comparison with experimental data. *International Journal of Marine Energy*, 14, 2016.

[42] Alexander J. Wagner and Ignacio Pagonabarraga. Lees–edwards boundary conditions for lattice boltzmann. *Journal of Statistical Physics*, 107(1):521–537, Apr 2002.

[43] Zeli Wang, Jianren Fan, and Kun Luo. Combined multi-direct forcing and immersed boundary method for simulating flows with moving particles. *International Journal of Multiphase Flow*, 34(3):283 – 302, 2008.

[44] Jie Wu and Chang Shu. A coupled immersed boundary–lattice boltzmann method and its simulation for biomimetic problems. *Theoretical and Applied Mechanics Letters*, 5(1):16 – 19, 2015.

[45] Guofeng Zhou, Limin Wang, Xiaowei Wang, and Wei Ge. Galilean-invariant algorithm coupling immersed moving boundary conditions and Lees-Edwards boundary conditions. *Physical Review E - Statistical, Nonlinear, and Soft Matter Physics*, 2011.